

Simple Giant Magnetoresistance Probe Based Eddy Current System of Defect Characterization for Non-Destructive Testing

Dalal Radia Touil¹, Ahmed Daas², Bachir Helifa¹, Ahmed Chaouki Lahrech¹, Lefkaier Ibn Khaldoun¹

¹Materials Physics Laboratory, Amar Telidji University of Laghouat, BP 37G Laghouat, 03000, Alegria

²LGP Laboratory, Laghouat University, BP 37G Laghouat, 03000, Algeria

Corresponding author: First A. Author (e-mail: dtouil993@gmail.com).

ABSTRACT The purpose of this paper is to present a new giant magnetoresistance (GMR) sensor in the eddy current testing technique for surface defect detection in conducting materials we show that the giant magnetoresistance -based eddy currents probe is more sensitive than the inductive probe with a difference of 80 %. A flat coil mounted on a ferrite pot is used to produce an alternate magnetic field, which gives rise to eddy currents in the material under test. Aluminum plates used with defects have nominal depths, widths, and lengths. The defects were scanned with the sensing axis perpendicular to the defect length. Two parameters were extracted from the giant magnetoresistance output voltage signal were obtained, and a simple correlation between the defect's dimensions and the giant magnetoresistance output voltage was proposed.

INDEX TERMS Giant magnetoresistance, Eddy current testing, Non-destructive testing, Crack Detection

I. INTRODUCTION

Eddy current non-destructive testing (ECNDT) has proven to be a reliable and rapid, and effective method for detecting defects such as fatigue cracks, inclusions, voids, and corrosion that occur in conductive materials. High sensitivity and low costs are the main parameters required for this method [1] hence the need for high-performance sensors.

The delicate measurement of crack location is difficult and has been the field of study of several researchers [2]. To improve the performance of the inspection of metallic structures using Eddy Current Testing (ECT) [3], the probe with the best characteristics [4], excitation signals methods [5] are still under investigation [3], and signal processing techniques [6]. Generally, Eddy Current Testing used with high-frequency magnetic fields [7], with inductive sensors is the most commonly used in many measurement systems, including Eddy Current non-destructive testing. The main disadvantage of induction coils is that their output voltage is proportional to the rate of change of the magnetic flux density, which limits their sensitivity at low frequencies. The part between over-current and over-voltage remains an open question for design/manufacturing electronic engineers. Preliminary studies are proposed for understanding the origin and the impact of this outstanding phenomenon [8], [9]. Therefore detection of deep flaws is

difficult with induction sensors [7]. As a consequence, other sensitive sensors of weak magnetic fields are required [10], [11], in our system, we test defects in Aluminum samples and use a giant magnetoresistance (GMR) and inductive sensors, and a lock-in amplifier in a low-frequency magnetic field. Giant magnetoresistance sensors are becoming of great interest nowadays thanks to their high frequency-independent sensitivity to the magnetic field, the small dimensions, the simplicity in use, and low power consumption, the giant magnetoresistance sensors detect the component of the magnetic field vector along their sensing axis.

In this work, a new mono-element giant magnetoresistance (GMR) sensor design suggested scanning large volumes of samples this mono-element GMR sensor is used with an excitation coil mounted on a ferrite pot to increase the sensitivity of the probe was able to detect deep cracks. In the present study, we use a ferrite coil alone. After, we compare the results with the output signal of the GMR probe in the same condition experience, a criterion relating the sensitivity of the eddy current probe with the characteristics of the excitation coil, a relationship between the cracks depth and the parameters extracted from the giant magnetoresistance sensor proposed for the configuration and geometry of the probe.

II. DESIGN OF THE PROBE

Fig.1 shows the proposed probes. The Eddy Current probe is composed of a coil mounted on a ferrite pot with the giant magneto-resistance sensor located on the coil axis. The characteristics of the excitation coil manufactured by SCIENSORIA are given in (see Table I). We chose giant magneto-resistance AAH004 00E as a receptor because of the high sensitivity and the small size. Also, we used a coil with a ferrite pot core because the emitting magnetic field produced increases in the middle.

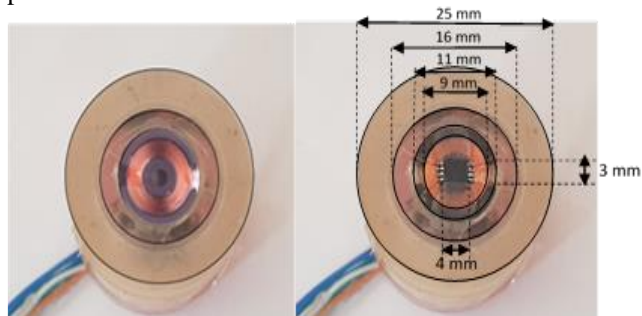


FIGURE 1. Inductive and giant magneto-resistance probes.

TABLE I. Characteristics of the excitation coil

Designation	Dimension Coil	
A flat coil mounted on ferrite pot	Inside radius	4.7 mm
	Outside radius	9 mm
	Length of coil	2.2mm
	Number of turns	175
	Number of layers	14
	Diameter of wire	0.14 mm
Ferrite pot size		
	Material	T6
	Core diameter	4.6mm
	Internal ring diameter	9.1mm
	Internal height	2.5mm
	Permeability	$\mu_r = 4000 \pm 25\%$

A. GIANT MAGNETORESISTANCE SENSOR CHARACTERISTICS

A giant magneto-resistance sensor of the type AAH004-00 manufactured by NVE Corporation used according to the catalog, their characteristics are presented in (Table II).[12]

TABLE II. Characteristics of the Giant Magneto-resistance

Designation	Characteristics and Package	
Giant magneto-resistance NVEAAH004	Saturation	1.5 mT = 15 Oe
Forfait (Package) MSOP	Sensitivity	32-48 V / T / V
Taille (Die size) μm	Linear Range	0.15 and 0.75 mT
411x1458	Resistance	2K $\Omega \pm 20\%$
	Power supply	9 V
	Package	MSOP8

The giant magneto-resistance sensor consists of four resistors in a Wheatstone bridge with two as sensing elements and the other two as dummy resistors magnetically shielded by a layer of a material with high magnetic permeability. Fig.2 depicts the internal configuration of the giant Magneto-resistor sensor

AAH004-00 produced by non-volatile electronics. Four giant magneto-resistors connected in a bridge configuration, with two of them magnetically shielded.

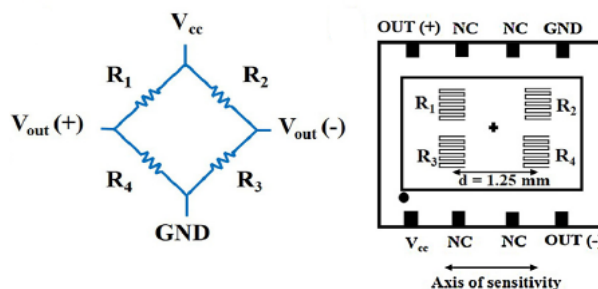


FIGURE 2. Giant magneto-resistor bridge sensor. [12]

The sensing axis of the giant magneto-resistance (GMR) is coplanar with the inspected surface, the excitation field on the coil axis is perpendicular to the sensing axis of the giant magneto-resistance probe and perpendicular to the plate, Once the GMR is close to or on top of a defect, the eddy current flow path is altered, which changes the applied magnetic field due to variation of the mutual inductance between eddy currents and the excitation coil.

The Giant magneto-resistance Magnetic Field Sensors can effectively sense the magnetic field generated by a current. Fig.3 below illustrates the sensor package orientation to detect the field from a current-carrying wire. It can be located above or below the chip, as long as it is oriented perpendicular to the sensitive axis. [12] it is depicting the sensitivity direction of the giant magneto-resistance sensor.

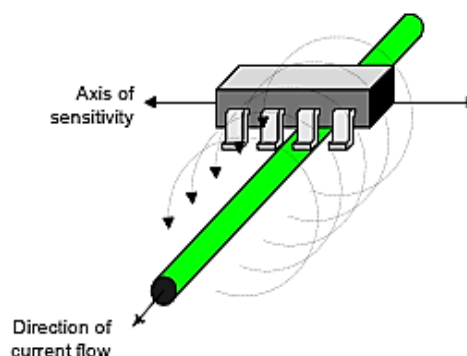


FIGURE 3. Sensing magnetic field from a current-carrying wire.[12]

Fig. 4 shows the sensor response as measured in the laboratory; the earth's magnetic field was not compensated during measurements.

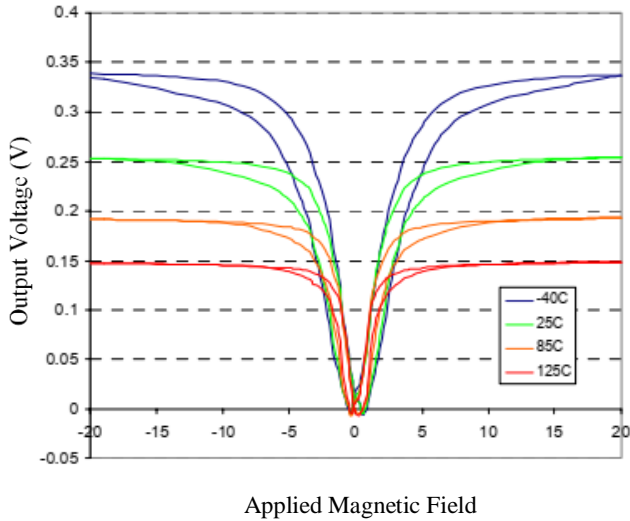


FIGURE 4. Output voltage of the magnetic sensor changed with the external magnetic field in different temperatures, 5v supply. [12]

The output voltage equation of the giant magnetoresistance used:

$$\Delta U = S_{eff} \cdot B \quad (1)$$

Where S_{eff} is the effective sensitivity, which is the multiply of the medium sensitivity and the supply voltage. For an AAH004-00E GMR sensor, $S_m=32-48$ (mV/V/mT), and a supply voltage $V_s = 9$ (V), depicted in table 2. [12] B magnetic field “flowing” through the surface of the giant magnetoresistance sensor.

III. ALUMINIUM ALLOY SAMPLE

In this study, an aluminum alloy sample was fabricated by laser devices μ Scan 6.5, the size of the sample shown in Figure 6 was 165x80 mm (testing by profilometer). Ten surface flaws can be seen extending from the edges of the sample, defects having nominal depths of 1, 2, 3, 4, 5, 6, 7, 8, 9 and 10 mm and widths of 0.67, 0.68, 0.68, 0.69, 0.65, 0.62, 0.57, 0.47, 0.61 and 0.55 mm, and the length was about 1.00, 2.00, 3.04, 4.03, 4.95, 5.43, 6.05, 7.65, 8.18, and 8.94mm, respectively, the sample depicted in Fig. 5.

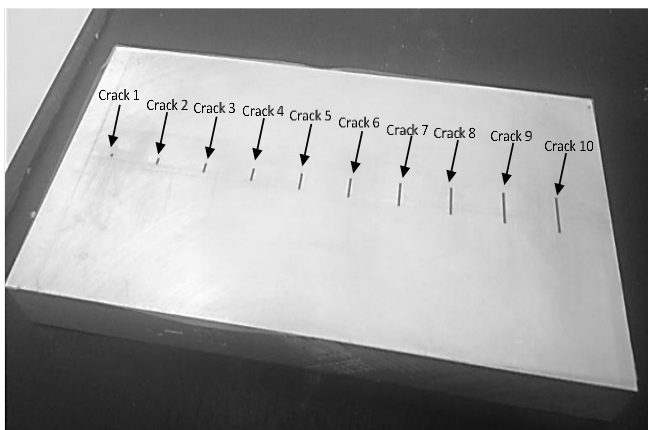


FIGURE 5. Aluminium plate using.

IV. EXPERIMENTAL SETUPS OF EDDY CURRENT SYSTEM

Fig.6 depicts the Schematization of the measurement system explained in the Block diagram of the experimental setup for the Eddy current measurements. A lock-in amplifier HF2LI is used to improve the signal-to-noise ratio. A sinusoidal voltage signal is selected with a Lock-in amplifier of 1 Vpp and different frequencies this signal is sent to the excitation coil and thus generates an AC-magnetic field.

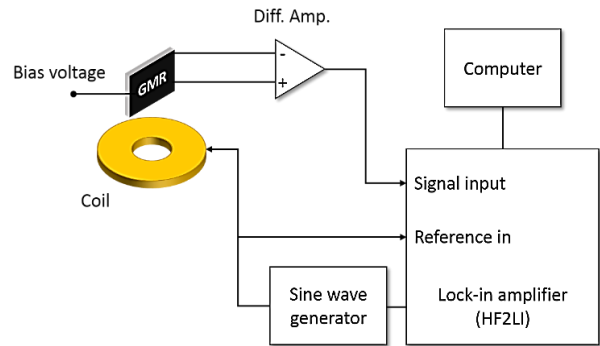


FIGURE 6. Schematization of the measurement system.

The component of the magnetic field induced by the eddy current in the Aluminum Alloy testing sample was measured by the sensor located down in the center of the coil. The giant magnetoresistance sensor response as well as the reference signal used by the lock-in amplifier to determine the amplitude.

Fig.7 shows the experimental setup, an Aluminum plate with cracks of different depths inspected using an eddy current testing system with a giant magnetoresistance sensor. In this experiment, eddy current probes are scanned over the surface of the aluminum plates in the direction of the giant magnetoresistance sensing axis perpendicular to the sample because it is the region where the maximum perturbation of the x component of the magnetic field (B_x) occurs.[10]

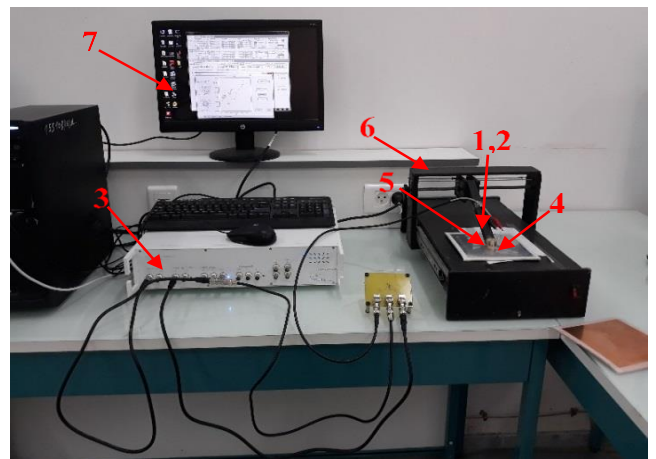


FIGURE 7. Measuring System. 1- Sensor (Ferrite Coil), 2- Sensor (Giant Magnetoresistance), 3- Lock-in Amplifier HF2LI, 4- Test Sample, 5- Cracking Opening, 6- Sensor Displacement System, 7- Pc-Interface.

The general procedure is to scan the area including the crack with a giant magnetoresistance probe the measurement depicted in Fig. 8, the sample depicted in Fig.5.

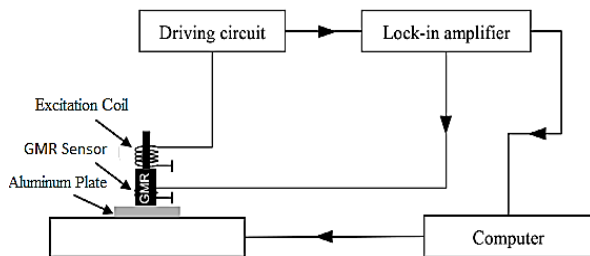


FIGURE 8. Schematic of the experimental setup for the eddy current testing system with giant magnetoresistance probe.

The same excitation coil was used for the same measurement the results include the variations of the tension records in the scan area, it is useful information about the cracks characterization. The sensor has an active area of about 100 by 200 mm in the middle of the layout[13], and the lift-off of the active area of the giant magnetoresistance sensor is approximately 0.5 mm. [7]

V. RESULTS & DISCUSSION

Fig.9 depicts the scan tests performed to evaluate the conditions of the material one surface crack its length is about 14 mm, width, and depth 1 mm, 5 mm. respectively, it was machined in the Aluminum plate with a thickness of 20 mm.



FIGURE 9. Schematic of the scanning tests.

An increase in the output voltage of the giant magnetoresistance and inductive probes was observed when the sensor moved on the top of the crack after further movement of the output voltage sensor came back to the nearly previous value. Fig.10 depicted the largest increase in amplitude observed with the giant magnetoresistance sensor compared with the inductive sensor. Which confirms the high sensitivity of the giant magnetoresistance probe.

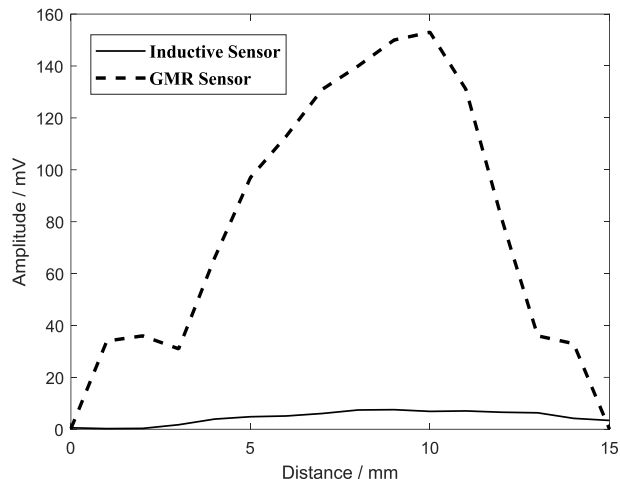


FIGURE 10. Giant magnetoresistance and inductive output voltage.

After that, we repeat the experiment, but we chose a scanning excitation frequency range of 20 kHz–160 kHz, and we compare the signal amplitudes of the flaws. The frequency scanning results for the crack shows in Fig. 11.

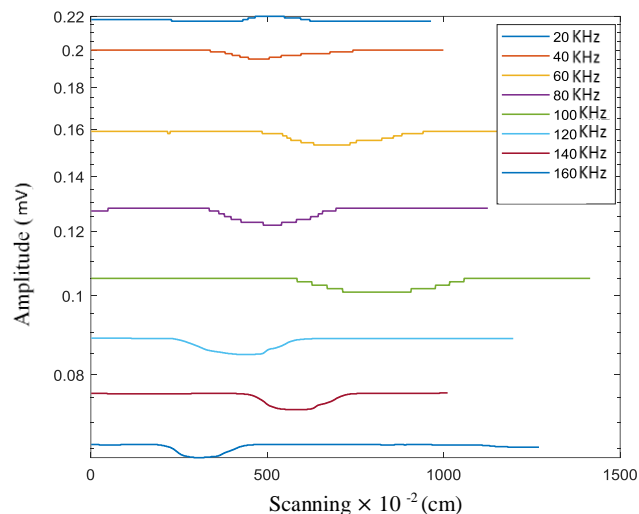


FIGURE 11. Results of the frequency scanning experiment for the eddy current testing system with inductive sensor.

To determine the optimum excitation frequency of the eddy current testing system with the giant magnetoresistance sensor, we chose the same scanning excitation frequency range. The results show in Fig.12.

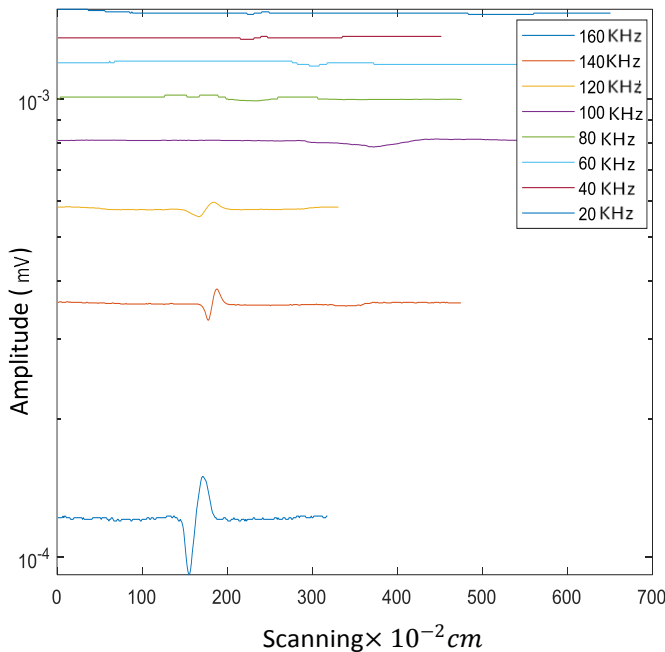


FIGURE 12 Results of the frequency scanning experiment for the Eddy current testing system with giant magnetoresistance sensor.

The results reveal that as the scanning frequency changed, the signal contrast between the flaw and non-flaw positions gradually changed and tended toward a stable level if the sample was without cracks, with no significant output variation measured.

The scanning results depicted in Fig.11 showed that the inductive probe possessed high sensitivity when we applied a very high frequency, close to the resonance frequency. Other than the giant magnetoresistance probe possessing high sensitivity when we applied weak frequencies, it will be less sensitive to the high frequencies. The schematization of the Aluminum plate present in Fig.13 shows the direction of the scanning tests performed along with the sample.

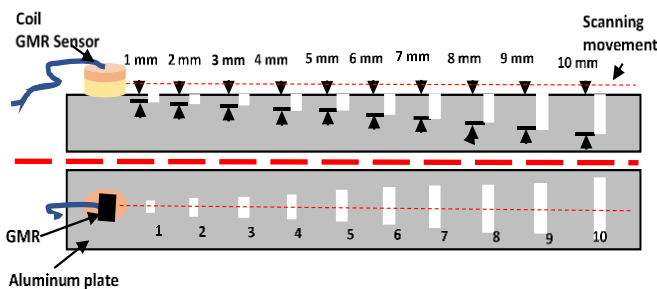


FIGURE 13 Representation of the performed scan: (a) Side view; (b) Top view.

Fig.14 shows typical giant magnetoresistance output signals of cracks at 20 kHz frequency when the scanning tests are performed along with the sample.

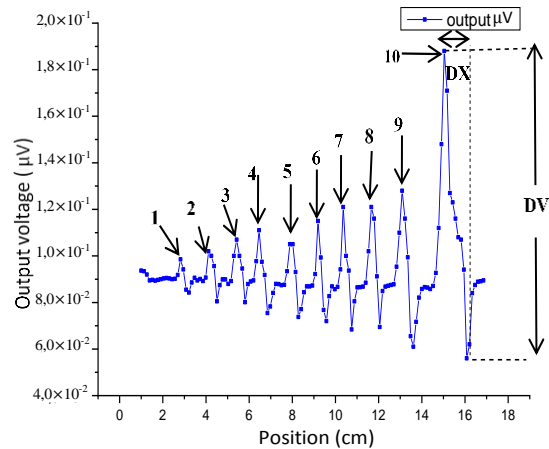


FIGURE 14 Results Typical giant magnetoresistance voltage of cracks for the 10 nominal depths which are $d=1, 2, 3, 4, 5, 6, 7, 8, 9, 10$ mm for each nominal width: $w_1=0.67$ mm, $w_2=0.68$ mm, $w_3=0.68$ mm, $w_4=0.69$ mm, $w_5=0.65$ mm, $w_6=0.62$ mm, $w_7=0.57$ mm, $w_8=0.47$ mm, $w_9=0.61$ mm, $w_{10}=0.55$ mm.

To analyze the probe response and correlate it with the crack depth and width. The average width (ΔX) and the average depth (ΔV) are two parameters that were defined and their values extracted from the giant magnetoresistance signal, the average depth is defined as the voltage difference between the maximum and minimum values of the output signal.

While the average width is defined as the difference in position between them. This method is used by some researchers to extract the limits of the sensitivity of eddy current testing systems, for cases, when the crack is scanned with the giant magnetoresistance sensing axis perpendicular to the crack length. Fig.15 shows the average width as a function of crack depth.

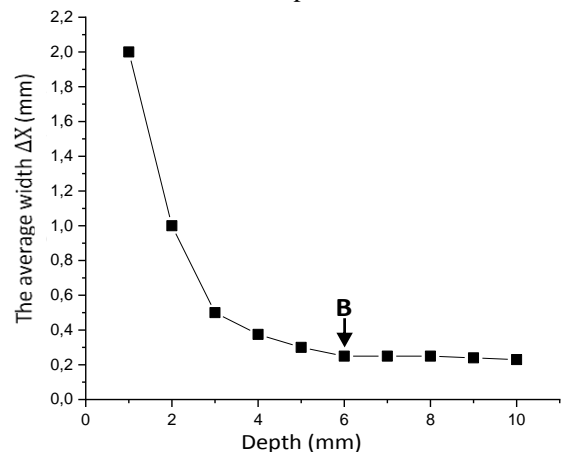


FIGURE 15 The average width as a function of the crack depth.

The average width is very sensitive to the crack depth smaller than 6 mm it's inversely proportional to the crack depth but for depth values greater than 6 mm, it's almost constant.

The first zone is highly sensing to the depths means that a mono sensor wipes a large volume from the sample we

don't need many sensors to scan a large sample, the characteristics of the excitation coil are very important to increase the sensitivity of the system, the Narrow of this zone is an issue treated in the continuous investigation.

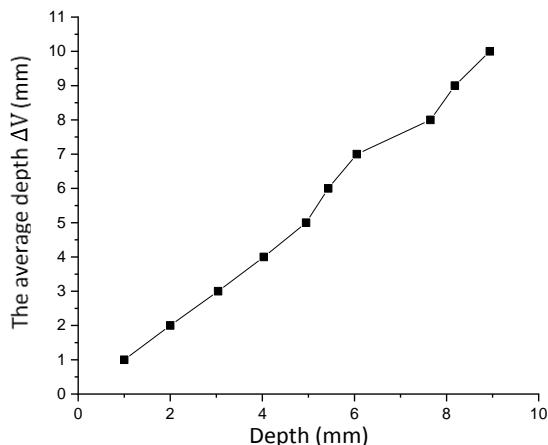


FIGURE 16 The average depth as a function of the crack depth.

We note that the experimental values of the average depth as a function of crack depth in Fig. 16 increase rapidly for cracks with depths smaller and greater than 6 mm.

VI. CONCLUSION

A new design of an eddy current mono-element giant magnetoresistance (GMR) probe is proposed the experimental results reveal that the sensor can control a large volume from the scanning sample.

Comparing the results of the inductive coil eddy current testing system with those of the high sensitivity GMR sensor eddy current testing (ECT) system, we conclude that the inductive coil produces had a good sensitivity at high frequencies.

But the high sensitivity magnetic sensor ECT system becomes good at low frequency.

The giant magnetoresistance-based eddy currents probe is more sensitive than the inductive probe. The design and realization of non-destructive eddy current testing effectively and the sensor gives accurate results.

The results confirmed that the average width depends on the crack depth and width but is more sensing to the width. As well as, the average depth is more sensitive to the depth but it's unlimited for depths greater than 6 mm.

A criterion is proposed based on the physical characteristics of the excitation coil, which helps increase the detection sensitivity of the system. We note that the experimental values of the average depth as a function of crack depth in Fig.16 increase rapidly for cracks with depths smaller and greater than 6 mm.

REFERENCES

- [1] D. Pasadas, T. J. Rocha, H. G. Ramos, and A. L. Ribeiro, "Evaluation of portable ECT instruments with positioning capability," *Measurement*, vol. 45, no. 3, pp. 393–404, Apr. 2012, doi: 10.1016/j.measurement.2011.11.005.
- [2] M. Pattabiraman, R. Nagendran, and M. P. Janawadkar, "Rapid flaw depth estimation from SQUID-based eddy current nondestructive evaluation," *NDT & E International*, vol. 40, no. 4, pp. 289–293, Jun. 2007, doi: 10.1016/j.ndteint.2006.12.003.
- [3] N. Yusa, Y. Sakai, and H. Hashizume, "An eddy current probe suitable to gain information about the depth of near-side flaws much deeper than the depth of penetration," *NDT & E International*, vol. 44, no. 1, pp. 121–130, Jan. 2011, doi: 10.1016/j.ndteint.2010.10.003.
- [4] H. Yamada, T. Hasegawa, Y. Ishihara, T. Kiwa, and K. Tsukada, "Difference in the detection limits of flaws in the depths of multi-layered and continuous aluminum plates using low-frequency eddy current testing," *NDT & E International*, vol. 41, no. 2, pp. 108–111, Mar. 2008, doi: 10.1016/j.ndteint.2007.08.004.
- [5] A. Simm, T. Theodoulidis, N. Poulakis, and G. Y. Tian, "Investigation of the magnetic field response from eddy current inspection of defects," *Int J Adv Manuf Technol*, vol. 54, no. 1–4, pp. 223–230, Apr. 2011, doi: 10.1007/s00170-010-2919-5.
- [6] D. J. Pasadas, A. L. Ribeiro, T. J. Rocha, and H. G. Ramos, "Open crack depth evaluation using eddy current methods and GMR detection," in *2014 IEEE Metrology for Aerospace (MetroAeroSpace)*, Benevento, Italy, May 2014, pp. 117–121. doi: 10.1109/MetroAeroSpace.2014.6865905.
- [7] E. Ramirez-Pacheco, J. H. Espina-Hernandez, F. Caleyo, and J. M. Hallen, "Defect Detection in Aluminium with an Eddy Currents Sensor," in *2010 IEEE Electronics, Robotics and Automotive Mechanics Conference*, Cuernavaca, Mexico, Sep. 2010, pp. 765–770. doi: 10.1109/CERMA.2010.91.
- [8] F. Zhu, B. Ravelo, F. Fouquet and M. Kadi, "Electrical predictive model of Zener diode under pulsed EOS", *Electronics Letters*, Vol. 51, No. 4, Feb. 2015, pp. 327-328.
- [9] F. Zhu, F. Fouquet, B. Ravelo, M. Kadi and A. Alaeddine, "Experimental investigation of Zener diode reliability under pulsed Electrical Overstress (EOS)", *Microelectronics Reliability*, Vol. 53, No. 9–11, Sept.–Nov. 2013, pp. 1288–1292.
- [10] Z. Zeng et al., "EC-GMR Data Analysis for Inspection of Multilayer Airframe Structures," *IEEE Trans. Magn.*, vol. 47, no. 12, pp. 4745–4752, Dec. 2011, doi: 10.1109/TMAG.2011.2160553.
- [11] D. He, Z. Wang, M. Kusano, S. Kishimoto, and M. Watanabe, "Evaluation of 3D-Printed titanium alloy using eddy current testing with high-sensitivity magnetic sensor," *NDT & E International*, vol. 102, pp. 90–95, Mar. 2019, doi: 10.1016/j.ndteint.2018.11.007.
- [12] www.nve.com [cited 2021 January 4]. Available from: <https://www.nve.com/Downloads/catalog.pdf>
- [13] T. Dogaru and S. T. Smith, "Giant magnetoresistance-based eddy-current sensor," *IEEE Trans. Magn.*, vol. 37, no. 5, pp. 3831–3838, Sep. 2001, doi: 10.1109/20.952754.